Mixed-State Specific Heat of the Type-II Superconductor $Nb_{0.77}Zr_{0.23}$ in Magnetic Fields up to B_{c2}

Mirmefstein, A.; Junod, Alain; Walker, Eric; Revaz, Bernard; Genoud, Jean-Yves; Triscone, Gilles

How to cite

MIRMEFSTEIN, A. et al. Mixed-State Specific Heat of the Type-II Superconductor $Nb_{0.77}Zr_{0.23}$ in Magnetic Fields up to B_{c2}. In: Journal of Superconductivity, 1997, vol. 10, n° 5, p. 527–535. doi: 10.1007/BF02767690

This publication URL: https://archive-ouverte.unige.ch/unige:121534
Publication DOI: 10.1007/BF02767690

Journal of Superconductivity, Vol. 10, No. 5, 1997

Mixed-State Specific Heat of the Type-II Superconductor $Nb_{0.77}Zr_{0.23}$ in Magnetic Fields up to B_{c2}

A. Mirmelstein,[1,2] A. Junod,[1] E. Walker,[1] B. Revaz,[1] J. Y. Genoud,[1,3] and G. Triscone[1]

Received 20 May 1997

In order to document the behavior of the mean-field mixed-state specific heat of an isotropic, strongly type-II superconductor (i.e., with a large value of the Ginzburg parameter κ), and to provide a basis for comparison with high-temperature superconductors, we measured the specific heat C of the alloy $Nb_{0.77}Zr_{0.23}$ with $T_c = 10.8$ K, $B_{c2}(0) = 7.9$ T, in magnetic fields $B =$ 0, 0.2, 1.0, 1.2, 2.0, 2.4, 3.0, 3.3, 4.0, 4.4, 4.8, 5.2, 6.0, 6.6, 7.2 and 10 T. The values of the upper critical field $B_{c2}(T)$, thermodynamic critical field $B_c(T)$, Ginzburg parameter $\kappa(T)$, and coefficient $\gamma(B) = \lim_{T\to 0}(C(T, B)/T)$ are derived from the specific heat data and found to be in agreement with the GLAG theory in the dirty limit. The behavior of the mixed-state specific heat is analyzed in terms of C_{el}/T, $\partial(C_{el}/T)/\partial B$, and $\partial(C_{el}/T)/\partial T$ vs. T curves, where C_{el} is the electronic contribution to the specific heat.

KEY WORDS: Type-II superconductivity; mixed state; specific heat; $Nb_{1-x}Zr_x$.

1. INTRODUCTION

Specific heat is one of the few bulk thermodynamic probes of the superconducting state, and as such was studied extensively in both classic and high-temperature superconductors. In classic superconductors, i.e., those studied before 1986, with critical temperatures T_c not exceeding 23 K, heat capacity measurements established the existence of a gap in the electronic density of states (DOS) at the Fermi level, of the order of $\Delta(0) \cong 3.5 k_B T_c$, showed an almost ideal example of a mean-field, second-order transition occurring at T_c, with a specific heat jump on the order of $\Delta C(T_c) \cong 1.4\gamma T_c$, and generally allowed one to correlate qualitatively the electron and phonon density of states and the critical temperature as predicted by the BCS theory [1], taking into account suitable corrections for retardation effects [2,3]. The required functionals of the electron and phonon DOS, i.e., the Sommerfeld constant γ, the Debye temperature $\Theta(T\to 0)$, and various moments $\langle \omega^n \rangle$ of the phonon DOS $F(\omega)$, could be extracted from the specific heat curves in the normal state (see, e.g., [4]). Magnetic fields were mostly applied for this purpose, to extend the normal-state data below T_c when simple extrapolations were unreliable. Although this method is useful for type-I superconductors, the T_c suppression does not exceed 0.38 K per Tesla for paramagnetically limited type-II superconductors. Most measurements were performed below 8 T in reasonably priced Nb–Ti magnets; rare early measurements were accomplished in fields as high as ≈ 20 T [5,6]. As a result, the mixed state specific heat of extreme type-II superconductors cannot be considered as well documented experimentally, even in the classic case. On the theoretical side, expressions for the mixed-state specific heat were obtained only in the temperature limit $T \ll T_c$, reflecting a superconducting DOS localized in the vortex cores and growing linearly with the magnetic field B [7,8].

The discovery of high-temperature superconductors has led to a dramatic renewal of interest in type-II superconductivity, in particular the behavior

[1]Département de Physique de la Matière Condensée, Université de Genève, CH-1211 Genève 4, Switzerland.
[2]Present address: Institute for Metal Physics, Russian Academy of Sciences, 620219 Ekaterinburg, Russia.
[3]Present address: Industrial Research Limited, Gracefield Research Center, Material Physics, PO Box 31-310, Lower Hutt, New Zealand.

0896-1107/97/1000-0527$12.50/0

of thermodynamic quantities such as the magnetization and the specific heat. Considerable differences with respect to classic superconductors arise from the fact that the coherence length ξ is extremely small, approaching atomic dimensions, and anisotropic. Critical fields are now on the order of 10^2 to 10^3 T, and anisotropies are so large that some properties can be considered as two-dimensional; the coherence volume is so small that the mean-field behavior is lost, while critical fluctuations play an important role near the transition [9]. The origin of pairing is an unsettled question, and indirect information on its mechanism, such as the symmetry of the order parameter, have been vividly debated [10–13]. Although the shift of T_c caused by available fields is modest, it is found that the field nevertheless has a dramatic effect on the specific heat anomaly at T_c and on the low-temperature specific heat. These effects are believed to convey fundamental information on the phenomenology of high-T_c superconductors, and detailed knowledge of the behavior of the mean-field component of the specific heat in the mixed state in the whole range of both temperature ($0 < T \leq T_c$) and field ($0 \leq B \leq B_{c2}$) is often required for the analysis of the experimental data.

Recently the specific heat of two classic type-II superconductors, $PbMo_6S_8$ and $NbSe_2$, was studied in magnetic fields up to 14 T [14–16]. $PbMo_6S_8$ is a Chevrel-phase, strongly coupled superconductor that approaches some microscopic parameters of high-T_c superconductors, such as the Fermi energy and the coherence length, but contrasts with its low anisotropy. Due to the very high value of the upper critical field $B_{c2}(0) = 52$ T [14,16] the normal-state specific heat cannot be measured directly. A conspicuous difference with the theoretical prediction [7,8] is the considerable reduction of the mixed-state "linear" term at low temperature: only half of the mean-field contribution $\gamma TB/B_{c2}$ is found at $T_c/10$. 2H-$NbSe_2$ is a layered compound that shows the effect of anisotropy on a type-II, strongly coupled superconductor. Due to the large coherence volume, superconducting fluctuations are not observable in zero field. The new feature found for this superconductor is the nonlinear growth of the mixed-state linear term with the field for $B > B_{c1}$ [15,16].

The aim of the present study is to document the behavior of the mean-field mixed-state specific heat of a strongly type-II (i.e., with a large value of the Ginzburg parameter κ), isotropic superconductor across the whole range of temperatures $0 < T \leq T_c$ and fields $0 \leq B \leq B_{c2}$. The bcc substitutional alloy system $Nb_{1-x}Zr_x$ has a maximum T_c of 10.8 K near $x = 0.25$ [17]. $Nb_{0.75}Zr_{0.25}$ is a strong coupling superconductor with $(dB_{c2}/dT)_{T_c} \approx -1$ T/K [18], gap ratio $2\Delta(0)/k_B T_c = 4.2$, thermodynamic critical field $B_c(0) = 0.25$ T, $\kappa \approx 20$, coherence length $\xi(0) = 64$ Å, Sommerfeld constant $\gamma \approx 9$ mJ/(K^2 g-at.), and atomic volume $V = 11.7$ cm^2/g-at. [4]. The coherence volume contains more than 10^4 atoms, and therefore superconducting fluctuations are not observable in zero field. Thus, it is a good candidate for our purpose. In this paper, we present specific heat measurements for a $Nb_{0.77}Zr_{0.23}$ sample with a very narrow zero-field superconducting transition in magnetic fields up to $B > B_{c2}$. The values of the upper critical field $B_{c2}(T)$, thermodynamic critical field $B_c(T)$, Ginzburg parameter $\kappa(T)$, and linear term coefficient $\gamma(B)$ are derived from the specific heat data and found to be in agreement with GLAG theory in the dirty limit. The behavior of the mixed-state specific heat is documented in terms of C_{el}/T, $\partial(C_{el}/T)/\partial B$, and $\partial(C_{el}/T)/\partial T$ vs. T curves, where C_{el} is the electronic contribution to the specific heat.

2. EXPERIMENTAL

The sample suitable for the purpose of the present study should have T_c near the maximum of the $Nb_{1-x}Zr_x$ system, and as narrow a superconducting transition as possible. This is not a trivial task due to peculiarities of the phase diagram [19]. The sample was selected from a series of specimens, including single crystals and ingots with various heat treatments. The chosen ingot with composition $Nb_{0.77}Zr_{0.23}$ was produced by electron bombardment zone melting in vacuum. The cooling was rapid enough to prevent the precipitation of the α-phase, which is a sluggish process. A small piece of the ingot was cut and probed by ac susceptibility measurements in 0.1 Oe rms. The full width of the superconducting transition between the 10 to 90% levels did not exceed 60 mK (Fig. 1). A sample of 24.8 mg in mass was cut from the same ingot for heat capacity measurements.

The total specific heat C was measured between 1.3 and 20 K in magnetic fields of 0, 0.2, 1.0, 1.2, 2.0, 2.4, 3.0, 3.3, 4.0, 4.4, 4.8, 5.2, 6.6, 7.2, and 10 T by a relaxation technique. Details are given in [16]. The accuracy, controlled using different masses of Ag and Cu, is ±1 to ±2%, including all fields; the relative accuracy vs. field changes is better. Note that the field was applied or changed above T_c in order to ensure equilibrium conditions in the thermodynamic sense. Because the mixed-state magnetization is small, we do not make a distinction between B and $\mu_0 H$.

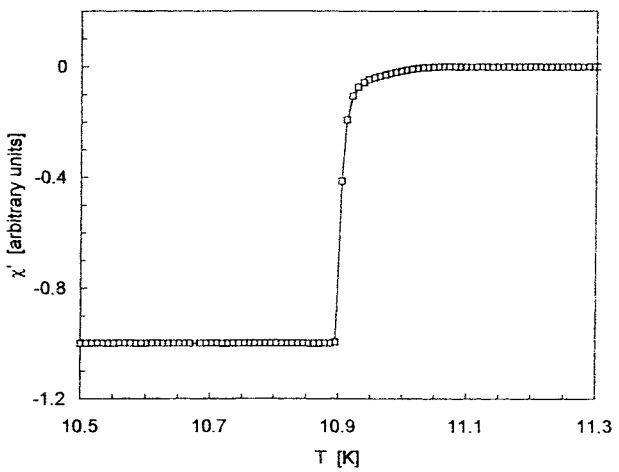

Fig. 1. AC susceptibility of the $Nb_{0.77}Zr_{0.23}$ sample measured in a field of 10 μT rms, 80 Hz.

3. RESULTS AND DISCUSSION

3.1. Mixed-State Specific Heat

Figure 2 shows the specific heat curves C/T vs. temperature squared for the $Nb_{0.77}Zr_{0.23}$ sample measured in different fields. In agreement with ac susceptibility measurements, the zero-field specific heat anomaly is ≈ 60 mK wide. Since the zero-field data obtained in the present study are in good agreement with previous specific heat measurements for a $Nb_{0.75}Zr_{0.25}$ polycrystal published in [4], where a full Eliashberg analysis of the zero-field specific heat was carried out, we shall concentrate here on the effect of the magnetic field. Basically, the field shifts the temperature of the specific heat step, reduces its amplitude, broadens the jump, and increases the

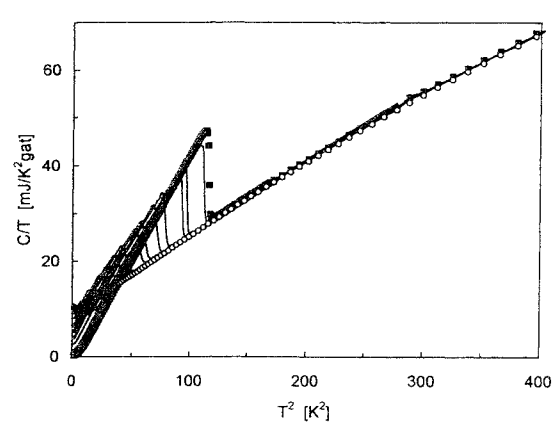

Fig. 2. Total specific heat C/T vs. T^2 up to 20 K for $Nb_{0.77}Zr_{0.23}$ in various fields $B=0$ (full squares), 0.2, 1.0, 1.2, 2.0, 2.4, 3.0, 3.3, 4.0, 4.4, 4.8, 5.2, 6.0, and 7.2 T (lines), and 10.0 T (open circles).

specific heat in the limit of low temperatures. For $B=7.2$ T, only traces of a superconducting transition are seen (Fig. 2), and at $B=10$ T the superconducting anomaly has completely disappeared. Above $T_c(B)$, the curves C/T vs. T^2 (or vs. T) for all fields coincide within experimental accuracy. Therefore, the specific heat measured at 10 T can be taken as the normal-state specific heat $C_n(T)$, thus giving the Sommerfeld constant $\gamma = 9.15 \pm 0.10$ mJ/(K^2 g-at.). It should be emphasized that downward integration of $\Delta C/T \equiv (C_s(T, B) - C_n(T))/T$ vs. T, where C_s is the specific heat in the superconducting state, results in $\Delta S \equiv S_s(T, B) - S_n(T) \to 0$ at $T \to 0$ within experimental uncertainty for all fields including $B=0$ (Table I, last two columns). This proves that the procedure that consists in applying or changing the field above T_c, in the normal state, ensures equilibrium conditions in the thermodynamic sense.

Figure 3 shows the electronic specific heat for the sample under study in the form $(C_s(T, B) - C_n(T))/T$ vs. T. Note that this is a straightforward difference between raw experimental points; the complication of phonon background subtraction is avoided. From the data of Fig. 3, we can immediately determine the behavior of the mixed-state specific heat in the low-temperature limit for all fields. At $T \approx T_c/10$, the only observable contribution is a mean-field, mixed-state linear term that grows almost proportionally to $B/B_{c2}(0)$, in agreement with theoretical predictions [7,8] (Fig. 4). At higher temperatures, the exponential rise of $C_s(T)$ is due to excitations across the temperature-dependent gap $\Delta(T)$.

Another characterization of the mixed-state specific heat that is directly measurable in a wide temperature range is given by the derivative of the specific heat with respect to magnetic field $\partial(C/T)/\partial B$, obtained by finite differences from consecutive fields (Fig. 5). Note again that no background subtraction is required to calculate this quantity because the lattice specific heat does not depend on B. For a classic type-II superconductor in the absence of thermal fluctuations, the field derivative of C/T is described phenomenologically by [16]

$$\frac{\partial(C/T)}{\partial B} \cong \frac{\gamma}{B_{c2}(0)} \vartheta(T - T_c(B)) + \gamma J(B) \frac{dT_c}{dB} \delta(T - T_c(B)) \qquad (1)$$

where $\vartheta(x) \equiv 1 - \int_{-\infty}^{x} \delta(x')\, dx'$ is the step function, and $J(B) \equiv (\Delta C/\gamma T)_{T_c(B)}$ is the dimensionless specific

Table I. Superconducting Transition Temperature T_c, Specific Heat Jump $(\Delta C/T)_{T_c(B)}$ (Idealized Value as Described in the Text), and Entropy of the Superconducting State S_s and Normal State S_n at a Temperature T_m Slightly Above $T_c(B)$ for $Nb_{0.77}Zr_{0.23}$ for Different Magnetic Fields[a]

B [T]	$T_{c,T}$ [K]	$T_{c,B}$ [K]	$\Delta C/T_c(B)$ [mJ/K² g-at.]	T_m [K]	$S_s(T_m)$ [mJ/K g-at.]	$S_n(T_m)$ [mJ/K g-at.]
0	10.79		21.0	11.010	173.80	173.59
0.1		10.68				
0.2	10.58		18.5			
1.0	9.86		15.5	10.250	152.49	152.71
1.1		9.75				
1.2	9.64		15.3			
2.0	8.85		13.5	9.351	130.66	130.52
2.2		8.66				
2.4	8.44		12.5			
3.0	7.84		11.1	8.263	106.81	106.91
3.15		7.65				
3.3	7.50		10.0			
4.0	6.71		8.7	7.508	93.24	92.48
4.2		6.49				
4.4	6.26		7.9	6.987	83.39	83.35
4.6		6.00				
4.8	5.77		6.4	7.102	85.65	85.76
5.0		5.51				
5.2	5.25		5.75	6.307	72.33	72.57
5.6		4.82				
6.0	4.20		4.2	5.827	65.18	65.28
6.3		3.78				
6.6	3.40		2.4	4.780	51.05	50.91
6.9		2.85				
7.2	2.5					

[a] $T_{c,T}$ and $T_{c,B}$ are determined by the position of the peaks in $\partial(C_{el}/T)/\partial T$ and $\partial(C/T)/\partial B$, respectively.

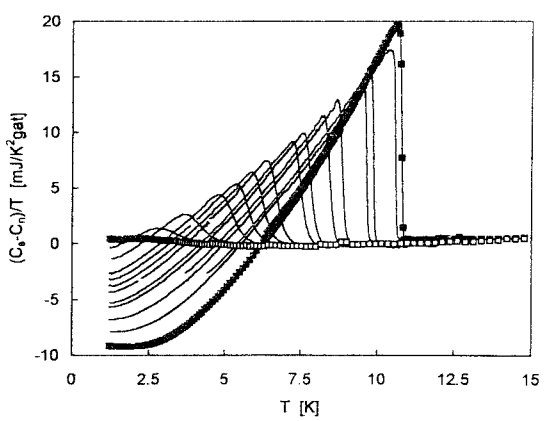

Fig. 3. Difference between the specific heat of $Nb_{0.77}Zr_{0.23}$ in the superconducting state and in the normal state measured in $B=10$ T vs. temperature T. The fields are $B=0$ (full squares), 0.2, 1.0, 1.2, 2.0, 2.4, 3.0, 3.3, 4.0, 4.4, 4.8, 5.2, 6.0 T (lines), and 7.2 T (open squares).

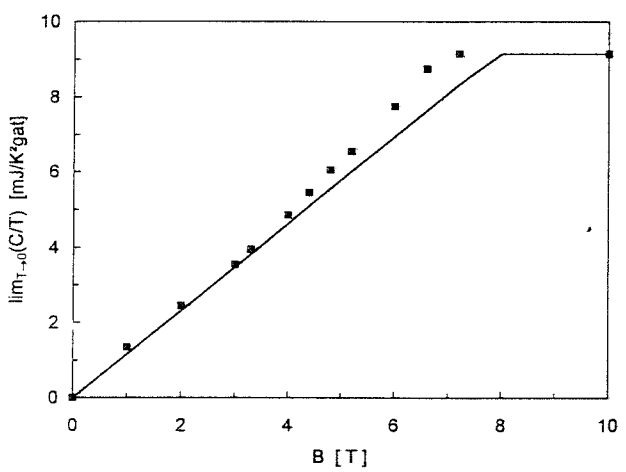

Fig. 4. Coefficient of the linear term of the specific heat in the mixed state in the low-temperature limit vs. magnetic field for $Nb_{0.77}Zr_{0.23}$. The full line represent $\gamma B/B_{c2}$.

heat jump, e.g., $J(0)=2$ in the two-fluid model. The first term represents the mixed-state contribution below $T_c(B)$ in the Maki–de Gennes approximation [7,8], and the second one accounts for the suppression of the jump $(\Delta C/T)_{T_c}$ over an infinitesimal temperature interval $\Delta T=\Delta B/(dB_{c2}/dT)$. The entropy increase from $T=0$ to $T>T_c(0)$ is left unchanged by the magnetic field. This constraint gives a relation

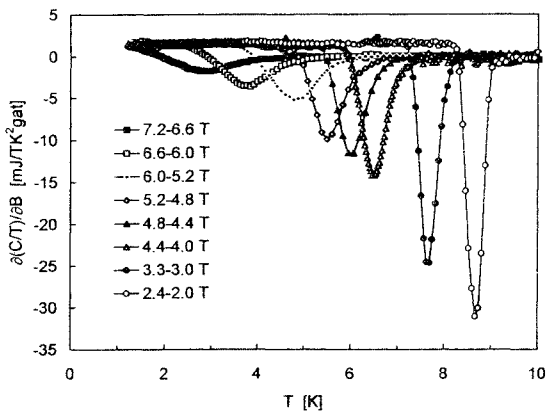

Fig. 5. Derivative of the specific heat C/T with respect to the magnetic field vs. temperature for $Nb_{0.77}Zr_{0.23}$. The derivative is obtained by finite differences from consecutive fields listed in the legend.

between the dimensionless jump $J(B)$ and the slope of the upper critical field:

$$J(B) \cong -\frac{T_c(B)}{B_{c2}(0)} \frac{dB_{c2}}{dT} \tag{2}$$

Therefore:

$$\frac{\partial(C/T)}{\partial B} \cong \frac{\gamma}{B_{c2}(0)} [\vartheta(T - T_c(B)) - T_c(B)\delta(T - T_c(B))] \tag{3}$$

This formula allows one to reconstruct the specific heat anomaly in zero field starting from the normal state at $B > B_{c2}(0)$, and summing up elementary contributions at lower fields:

$$\frac{C_{el}(T, B=0)}{T} = \gamma + \int_{B_{c2}(0)}^{0} \frac{\partial(C/T)}{\partial B} dB \tag{4}$$

Assuming, for example, a parabolic approximation for the temperature dependence of the upper critical field, $B_{c2}(T) = B_{c2}(0)(1 - t^2)$, one obtains $C(T, B = 0)/T = 3\gamma t^2$, $t \equiv T/T_c < 1$, which is the two-fluid model obeyed by many medium to strong coupling superconductors at not too low temperatures.

From Fig. 5, the field derivative of the specific heat in the mixed state $\partial(C/T)/\partial B$ is approximately equal to 1.5 mJ/(T K^2 g-at.) below the superconducting transition, and stays almost temperature and field independent, in conformity with Eq. (3). Thus, the mixed-state specific heat $C_s(T, B) - C_s(T, 0)/T$ is proportional to the magnetic field not only in the limit of low temperatures (Fig. 4), but also almost up to $T_c(B)$. Note that the dip of $\partial(C/T)/\partial B$ varies strongly with $T_c(B)$. Its amplitude (in units of mJ/(T K^2 g-at.)) can be approximated by $0.1T_c(B)^{2.65}$. According to Eqs. (1)–(3), the area under the dip should be proportional to $T_c(B)$ to preserve the conservation of entropy; consequently its width should vary as $T_c(B)^{-1.65}$. This agrees qualitatively with the observed broadening, the origin of which will be discussed later.

3.2. Determination of $T_c(B)$, $B_{c2}(T)$, and $B_c(T)$

In order to proceed further, we first determine the values of $T_c(B)$. The practical definition is not unique. The inflection point of the electronic specific heat, i.e., the temperature at which $\partial(C_{el}/T)/\partial T$ has its maximum negative value in the specific heat jump, defines $T_{c,T}(B)$ (Table I, first column). The position of the maximum negative value of $\partial(C/T)/\partial B$ (Fig. 5) gives another bulk determination $T_{c,B}(B)$ (Table I, second column). For the latter, it is not necessary to remove the lattice contribution. Both definitions of course coincide in the case of an ideally sharp second-order transition. As shown in Fig. 6, they do in practice within error limits, and allow a precise determination of the phase boundary in the (B, T) plane. The $B_{c2}(T)$ curve follows the theoretical WHH function in the dirty limit [20], thus confirming earlier findings [18]. The implicit WHH function in the case $\alpha = \lambda = 0$ is conveniently approximated by $B_{c2}(T)/B_{c2}(0) \cong (1-t^2)(1 - 1.181t^2 + 1.614t^3 - 0.712t^4)$, $t \equiv T/T_c$; in particular, $B_{c2}(0) = -0.693T_c(dB_{c2}/dT)|_{T_c}$. A fit to the experimental points yields the

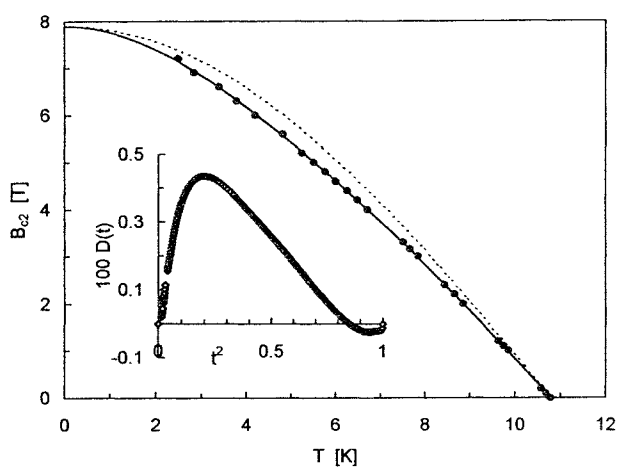

Fig. 6. Upper critical field as a function of temperature for $Nb_{0.77}Zr_{0.23}$ determined by the position of the peak of $\partial(C/T)/\partial B$ or $\partial(C_{el}/T)/\partial T$ (closed circles). The full line is a fit of the WHH function in the dirty limit, with $T_c = 10.79$ K and $B_{c2}(0) = 7.9$ T. The broken line represents $B_{c2}(T)$ in the BCS limit. Inset: deviation function of the thermodynamic critical field.

parameters $T_c = 10.79$ K and $B_{c2}(0) = 7.9$ T (full line in Fig. 6). Note that the experimental results depart from the BCS interpolation formula $B_{c2}(T) \cong \kappa B_c(0)(1-t^2)(1.77-0.43t^2+0.07t^4)$ [21] (dotted line in Fig. 6).

We can now examine the mixed-state specific heat in more detail. As pointed out in Section 3.1, in the low-temperature limit $\partial(C/T)/\partial B \approx \gamma/B_{c2}(0)$, so that $(C_s(T,B)-C_s(T,0))/\gamma T \approx B/B_{c2}(0)$, $B < B_{c2}(0)$, in close agreement with theory [7,8]. This contribution is understood as the specific heat of the nonsuperconducting electrons in the vortex cores. At somewhat higher temperatures, as can be seen from Fig. 5, $\partial(C/T)/\partial B$ is about 1.5 mJ/(T K^2 g-at.) $\approx 1.3\gamma/B_{c2}(0)$, so that $C_s(T,B)-C_s(T,0)/\gamma T \approx 1.3B/B_{c2}(0)$. In other words, the mixed-state specific heat is always proportional to $B/B_{c2}(0)$, whereas the prefactor is somewhat temperature dependent in the range where excitations across the gap become essential. We shall return to this point in Section 3.3.

The value of the specific heat jump $(\Delta C/T)_{T_c(B)}$ at different fields was obtained by extrapolations of C/T from above and from below $T_{c,T}(B)$, and by requiring that the entropy added just below $T_{c,T}(B)$ be equal to the entropy removed just above $T_{c,T}(B)$ (Table I, third column).

Having obtained T_c, the jump in zero field, and the normal-state specific heat, we can calculate the thermodynamic critical field $B_c(T)$:

$$B_c^2(T) = \frac{2\mu_0}{V}\int_T^{T_c} dT' \int_{T'}^{T_c} dT'' \frac{C_s(T'')-C_n(T'')}{T''} \qquad (5)$$

where $V = 11.7$ cm^3/g-at. is the atomic volume for $Nb_{0.77}Z_{0.23}$. The value of B_c at $T=0$ is 0.256 T. Its temperature dependence follows very closely the two-fluid parabolic law, with a maximum derivation $D(t) = B_c(T)/B_c(0) - (1-t^2) \cong +0.005$ at $t^2 = 0.2$ (Fig. 6, inset), in qualitative agreement with previous results [4]. In the weak-coupling, BCS case, the maximum deviation would be -0.037 at $t^2 = 0.49$.

3.3. Specific Heat Jump at $T_c(B)$ and Ginzburg Parameter $\kappa(T)$

We can now calculate the values of the Ginzburg parameters $\kappa_1(T)$ and $\kappa_2(T)$ in the notation of Eilenberger [22]:

$$B_{c2}(T) = \sqrt{2}\kappa_1 B_c(T) \qquad (6)$$

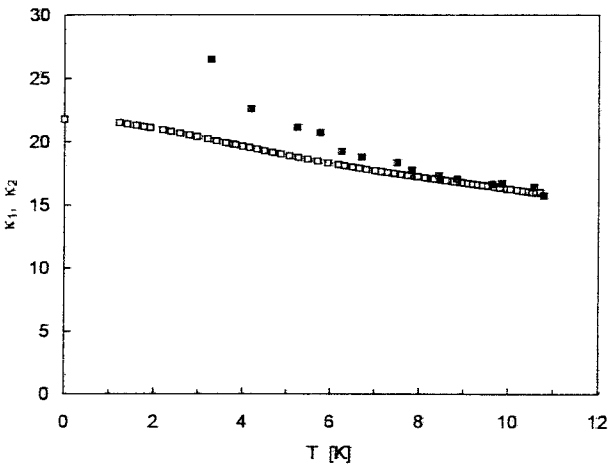

Fig. 7. Temperature dependence of the Ginzburg parameters κ_1 (open squares) and κ_2 (full squares) for $Nb_{0.77}Zr_{0.23}$, calculated using Eqs. (6) and (7), respectively.

$$\left(\frac{\Delta C}{T}\right)_{T_c(B)} = \frac{V}{1.16\mu_0(2\kappa_2^2-1)}\left(\frac{dB_{c2}}{dT}\right)^2 \qquad (7)$$

The temperature dependences of $\kappa_1(T)$ and $\kappa_2(T)$ are shown in Fig. 7. As expected [22], $\kappa_1(T)$ and $\kappa_2(T)$ tend to the same value at $T \to T_c$ when the electrodynamics of the superconducting state becomes fully local. As a consequence, the specific-heat jump at the transition from the normal state to the mixed state is reduced in amplitude with respect to the jump at the transition from the normal state to the superconducting state in $B=0$, which is given by Rutger's equation:

$$\left(\frac{\Delta C}{T}\right)_{T_c(0)} = \frac{V}{\mu_0}\left(\frac{dB_c}{dT}\right)^2_{T_c(0)} \qquad (8)$$

The value of the specific heat jump at the transition from the normal state to the mixed state is found to be proportional to $1-B/B_{c2}(0)$ for $0.2\text{ T} < B \le B_{c2}(0)$ (Fig. 8). The quantity $1-B/B_{c2}(0)$ can be visualized as the volume fraction of the sample that is locally superconducting, i.e., outside of the vortex cores counted with an effective area $2\pi\xi^2$. The difference between the zero-field and the in-field transitions shows up as an upturn at $B \to 0$ on the right of Fig. 8. This difference is also directly apparent in Fig. 3. The ratio between the zero-field jump and the in-field jump extrapolated to $B=0$ (full line in Fig. 8) is 1.16, in agreement with Eqs. (6)–(8). Note that the coefficient 1.16 arises for a triangular vortex lattice, i.e., when interactions between vortices are taken into account. The curve for the lowest nonzero field in

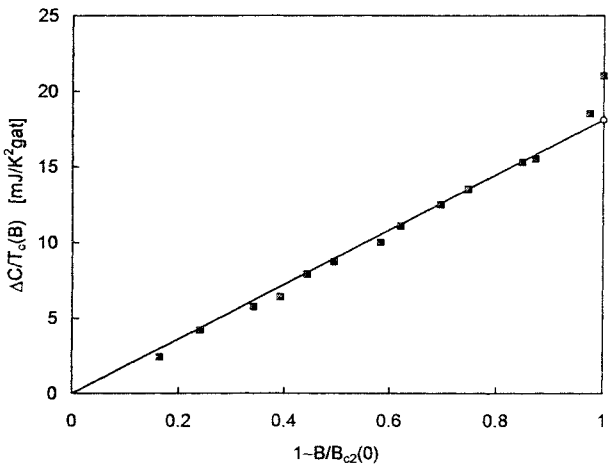

Fig. 8. Specific heat jump $(\Delta C/T)_{T_c(B)}$ vs. $1-B/B_{c2}(0)$ (full squares) for $Nb_{0.77}Zr_{0.23}$, all fields included. The open circle shows the value of the specific heat jump in $B=0$ divided by a factor 1.16. The line through the full symbols represents the dependence $(\Delta C/T)_{T_c(B)}=[(\Delta C/T)_{T_c(B=0)}/1.16][1-B/B_{c2}(0)]$.

these experiments ($B=0.2$ T) has an intermediate behavior. A similar dependence of the specific heat jump on the magnetic field was reported in [6] for Nb_3Sn.

As a matter of fact, the proportionality between the mixed-state specific heat and $1-B/B_{c2}(0)$ is not limited to the jump at $T_c(B)$. As shown in Fig. 9, the $\Delta C(T, B)/T$ vs. T curves for $B>0.2$ T can be collapsed over most of the intermediate temperature range by plotting $((C_s-C_n)/T)/(1-B/B_{c2}(0))$ vs. $T/T_c(B)$. In the low-temperature limit, this is a direct consequence of the Maki–de Gennes contribution

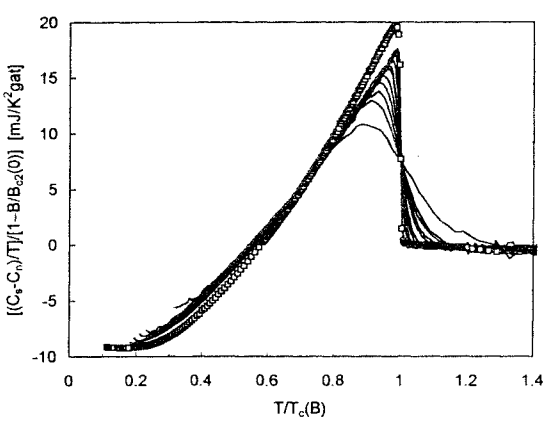

Fig. 9. Zero-field (open squares) and mixed-state (lines) electronic specific heat difference $(C_s(T, B)-C_n(T))/T\equiv\Delta C(T, B)/T$ in various magnetic fields for $Nb_{0.77}Zr_{0.23}$, normalized by the "effective superconducting fraction" $1-B/B_{c2}(0)$, vs. reduced temperature $T/T_c(B)$. The fields are $B=1.0$, 1.2, 2.0, 2.4, 3.0, 3.3, 4.0, 4.4, 4.8, 5.2, and 6 T.

with C_s/T proportional to $B/B_{c2}(0)$. Near T_c, the symmetry of the vortex lattice plays a role, as shown by the factor 1.16 that arises there. One sees that the magnetic field excludes some entropy from the transition region, which must be redistributed at lower temperature to obey the third law of thermodynamics. This causes a subtle change of the shape of the mixed-state specific heat. Even if the curves for $B>0.2$ T were rescaled by a factor 1.16, their normalized shape would differ from that of the $B=0$ curve. Formally, the collapse of the curves for $B>0.2$ T in Fig. 9 means that we can define a dimensionless scaling function f by

$$\frac{C_s-C_n}{\gamma T}=\left(1-\frac{B}{B_{c2}(0)}\right)f(t_B), \qquad t_B\equiv\frac{T}{T_c(B)} \tag{9}$$

which implies the following relation for the field derivative:

$$\frac{\partial}{\partial B}\left(\frac{C_s-C_n}{\gamma T}\right) = \frac{1}{B_{c2}(0)}\left[-f(t_B)+\frac{d\ln T_c(B)}{d\ln(B_{c2}(0)-B)}\,t_B\frac{df}{dt_B}\right] \tag{10}$$

The function f must have the property $f(0)=-1$, and consequently relation (10) includes the particular case $\partial(C/T)/\partial B=\gamma/B_{c2}$ at $T\to 0$. With some rather strong assumptions, e.g., the power laws $f(t_B)=3t_B^2-1$ and $B_{c2}(T)=B_{c2}(0)(1-t^2)$, this propriety would hold exactly up to T_c. If BCS functions were used both for f and $B_{c2}(T)$, $\partial(C/T)/\partial B$ would tend to zero at T_c, at variance with experiment. The experimental f in the present case is close to the average between the BCS and $3t_B^2-1$ functions, and $B_{c2}(T)$ follows the WHH dependence. In these conditions, Eq. (10), based on the observed scaling property, reproduces the smooth increase of $\partial(C/T)/\partial B$ from γ/B_{c2} at $T\ll T_c$ to ≈ 1.3 (γ/B_{c2}) in the mid-T_c range.

3.4. Broadening of the Superconducting Transition in a Magnetic Field

The broadening of the superconducting transition that results from the application of a magnetic field can be described by generalizing Eq. (3). The δ-function is replaced by its broadened counterpart:

$$\delta(T-T_c(B)) \to \frac{A}{\pi B^n}\frac{1}{1+x^2}, \qquad x\equiv A\frac{T-T_c(B)}{B^n} \tag{11}$$

The field dependence of the dip width in $\partial(C/T)/\partial B$ (Fig. 5) is described by an exponent n near 1.5 for $Nb_{0.77}Zr_{0.23}$. This leads us to conclude that the systematic broadening of the initially sharp transition, which simulates the effect of the fluctuations, results from local variations of the mean free path in the dirty limit. If broadening was due to thermal fluctuations of the order parameter, the typical transition width in a magnetic field of 4 T would be on the order of 60 mK, whereas the observed transition width is larger by an order of magnitude. Besides, fluctuation effects lead to exponents $n<1$ [16]. Alternatively, local variations of the mean free path lead to a corresponding distribution of the upper critical field ΔB_{c2} via a distribution of the Ginzburg parameter κ, while the thermodynamic critical field, i.e., the condensation energy, remains uniform throughout the sample. Such a broadening results in a field-dependent transition width $\Delta T_c(B)$ varying as

$$\frac{\Delta T_c(B)}{T_c(0)} = \frac{\Delta B_{c2}}{B_{c2}(0)} \left(-\frac{d \ln b}{dt} \right)^{-1}$$
$$b(t) \equiv \frac{B_{c2}(t)}{B_{c2}(0)} \tag{12}$$

The curves $\partial(C/T)/\partial B$ vs. T (Fig. 5) measured in various fields $B>2.4$ T collapse onto a single curve (Fig. 10) when they are normalized to their peak value and plotted as a function of $T-T_c(B)/\Delta T_c(B)$. The fact that they do does not depend on the value of ΔB_{c2}. The latter parameter is determined by the width of the common curve, with the result $\Delta B_{c2} \approx 1$ T. At lower fields, the experimental field mesh is too crude to allow a precise determination of $\partial(C/T)/\partial B$; but the same scaling holds at all fields ≥ 1 T for the equivalent plot of $\partial(C_{el}/T)/\partial T$, which may be calculated with a better resolution, but requires first the subtraction of the lattice contribution (Fig. 11).

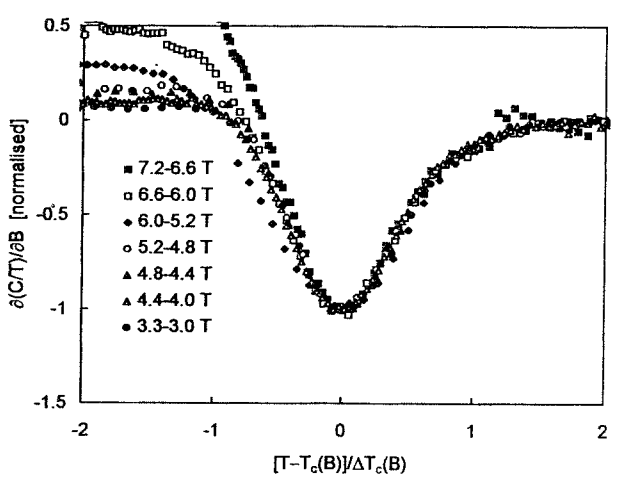

Fig. 10. Derivative of the total specific heat C/T with respect to the magnetic field near $T_c(B)$, normalized to -1 at the minimum, vs. reduced temperature $(T-T_c(B))/\Delta T_c(B)$, where $\Delta T_c(B)$ is given by Eq. (12).

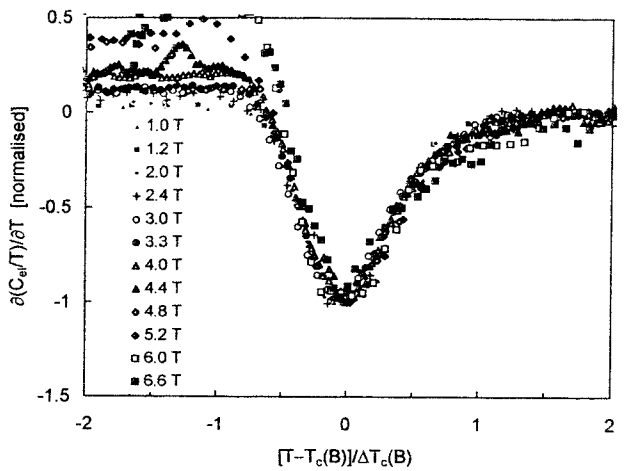

Fig. 11. Derivative of the electronic specific heat C_{el}/T with respect to temperature near $T_c(B)$, normalized to -1 at the minimum, vs. reduced temperature $(T-T_c(B))/\Delta T_c(B)$.

4. CONCLUSION

The behavior of the mixed-state specific heat of $Nb_{0.77}Zr_{0.23}$, which can be considered as a reference type-II classic superconductor (Table II), is documented in terms of $\Delta C/T$ vs. T and $\partial(C/T)/\partial B$ vs. T curves. The field causes a shift of the transition toward lower temperatures, and an increase of the electronic specific heat in the superconducting state. The bulk measurements of $T_c(B)$ by closely spaced specific heat experiments from 0 to $B_{c2}(0)=7.9$ T shows an almost perfect WHH [20] dependence. The difference between the transitions to the Meissner

Table II. Parameters Characterizing $Nb_{77}Zr_{23}$[a]

	$Nb_{75}Zr_{25}$ [4]	$Nb_{77}Zr_{23}$ (this work)
T_c (K)	10.78	10.79
V (cm^3/g-at.)	11.67	11.67
B_c (T)	0.249	0.256
B_{c2} (T)		7.9
$\kappa(0)$		21.8
$\kappa(T_c)$		15.9
γ (mJ/K^2 g-at.)	8.96	9.15
$\Delta C/\gamma T_c$	2.23	2.30

[a]See text for definitions. Estimated accuracy is ±1%.

state and to the Shubnikov state is observed. The systematic broadening of the initially sharp transition, which simulates the effect of fluctuations, results from local variation of the mean free path in the dirty limit. The mixed-state specific heat $(C_s(T, B) - C_s(T, 0))/\gamma T$ is proportional to $B/B_{c2}(0)$, in close agreement with theory [7,8], almost up to $T_c(B)$. This contribution at low temperature is understood as the specific heat of nonsuperconducting electrons in the vortex cores. Its extended validity almost up to T_c appears to be a particular property of moderately strong coupling superconductors.

ACKNOWLEDGMENTS

The authors are grateful to M. Decroux for ac susceptibility measurements, and to J. Muller and J. Sierro for useful discussions. This work was supported by the Fonds National Suisse de la Recherche Scientifique.

REFERENCES

1. J. Bardeen, L. N. Cooper, and J. R. Schrieffer, *Phys. Rev.* **108**, 1175 (1957).
2. W. L. McMillan, *Phys. Rev.* **167**, 331 (1968).
3. P. B. Allen and R. C. Dynes, *Phys. Rev. B* **12**, 905 (1975).
4. A. Junod, J.-L. Jorda, and J. Muller, *J. Low Temp. Phys.* **62**, 301 (1986).
5. G. R. Stewart and B. L. Brandt, *Phys. Rev. B* **29**, 3908 (1984).
6. M. N. Khlopkin, *Sov. Phys. JETP* **63**, 164 (1986).
7. C. Caroli, P. G. de Gennes, and J. Matricon, *Phys. Lett.* **9**, 307 (1964); *Phys. kondens. Mater.* **3**, 380 (1965).
8. K. Maki, *Physics* **1**, 21 (1964); **1**, 127 (1964).
9. M. B. Salamon, S. E. Inderhees, J. P. Rice, B. G. Pazol, D. M. Ginsberg, and N. Goldenfeld, *Phys. Rev. B* **38**, 885 (1988).
10. R. C. Dynes, *Solid State Commun.* **92**, 53 (1994).
11. J. R. Schrieffer, *Solid State Commun.* **92**, 129 (1994).
12. C. C. Tsuei, J. R. Kirtley, C. C. Chi, L. S. Yu-Jahnes, A. Gupta, T. Shaw, J. Z. Sun, and M. B. Ketchen, *Phys. Rev. Lett.* **73**, 593 (1994).
13. Ya. G. Ponomarev, N. B. Brandt, C. S. Khi, S. V. Tchesnokov, E. B. Tsokur, A. V. Yarygin, K. T. Yusupov, B. A. Aminov, M. A. Hein, G. Müller, H. Piel, D. Wehler, V. Z. Kresin, K. Rosner, K. Winzer, and Th. Wolf, *Phys. Rev. B* **52**, 1352 (1995).
14. D. Sanchez, Ph.D. thesis No. 2652 (University of Geneva, 1994), unpublished.
15. D. Sanchez, A. Junod, J. Muller, H. Berger, and F. Levy, *Physica B* **204**, 167 (1995).
16. A. Junod, in *Studies of High-Temperature Superconductors*, Vol. 19, A. V. Narlikar, ed. (Nova Science Publishers, New York, 1996), pp. 1–68.
17. J. K. Hulm and R. D. Blaugher, *Phys. Rev.* **123**, 1569 (1961).
18. L. J. Neuringer and Y. Shapira, *Phys. Rev.* **148**, 231 (1966).
19. R. P. Elliott, *Constitution of Binary Alloys*, First Supplement (McGraw-Hill, New York, 1965), p. 279.
20. N. R. Werthamer, E. Helfand, and P. C. Hohenberg, *Phys. Rev.* **147**, 295 (1966).
21. L. P. Gor'kov, *Zh. Eksp. Teor. Fiz.* **37**, 833 (1959) [*Soviet Phys. JETP* **37**(10), 593 (1960)].
22. G. Eilenberger, *Phys. Rev.* **153**, 584 (1967).